Evaluation of arsenic sorption and mobility in stream sediment and hot spring deposit in three drainages of the Tibetan ....

Article *in* Applied Geochemistry · April 2016

DOI: 10.1016/j.apgeochem.2016.04.006

CITATIONS
0

READS
136

5 authors, including:

Shehong Li

31 PUBLICATIONS **391** CITATIONS

SEE PROFILE

Yan Zheng

Columbia University

95 PUBLICATIONS **4,037** CITATIONS

SEE PROFILE

Applied Geochemistry 77 (2017) 89–101

Contents lists available at ScienceDirect

Applied Geochemistry

journal homepage: www.elsevier.com/locate/apgeochem

Evaluation of arsenic sorption and mobility in stream sediment and hot spring deposit in three drainages of the Tibetan Plateau

Yinfeng Zhang [a, b], Shehong Li [a, **], Lirong Zheng [c], Jingan Chen [a], Yan Zheng [d, e, *]

[a] State Key Lab of Environmental Geochemistry, Institute of Geochemistry, Chinese Academy of Sciences, Guiyang 550081, China
[b] University of Chinese Academy of Sciences, Beijing 100049, China
[c] Institute of High Energy Physics & Theoretical Physics Center for Science Facilities, Chinese Academy of Sciences, Beijing 100049, China
[d] Queens College, City University of New York, Flushing, NY 11367, United States
[e] Lamont-Doherty Earth Observatory, Columbia University, Palisades, NY 10964, United States

ARTICLE INFO

Article history:
Received 28 May 2015
Received in revised form
17 February 2016
Accepted 19 April 2016
Available online 21 April 2016

Keywords:
X-ray Absorption Spectroscopy
Arsenic
Hot spring
Salween
Yangtze
Mekong

ABSTRACT

Enrichment of arsenic (As) in sediment (12–227 mg/kg) in the upstream tributaries of the Indus and Brahmaputra Rivers originating from the Tibetan Plateau where hot springs were abundant has been found. Sandy sediment samples from the Nu-Salween River, Lantsang-Mekong River and Jinsha-Yangtze River also originating from the Tibetan Plateau were collected in July, 2012 and were found to contain 6.8 mg/kg to 30.5 mg/kg As (average17.3 ± 6.5 mg/kg, n = 12). Deposits collected within 1 m of two hot springs in Changdu, Tibet displayed significantly higher As levels: 263.7 mg/kg in LD-2 with 65% quartz and 101.8 mg/kg in NuD-1 with 82% calcite. To evaluate the valence states of As and also the phases responsible for sorption, X-Ray Absorption Spectroscopy (XAS) was employed to analyze the two hot spring deposits and three river sediment samples: coarse sand NuD-6 (As 14.6 mg/kg), fine sand NuD-4 (As 17.8 mg/kg), and silty sand LD-1 (As 30.5 mg/kg). The X-ray absorption near edge spectrum (XANES) data indicate that 70% of As from 3 samples in the Nu-Salween River drainage (NuD-1, NuD-4 and NuD-6) is As(V) or arsenate, with the rest being As(0) or As–Fe sulfides. The proportion of As(V) is 90% for 2 samples in the Lantsang-Mekong River drainage (LD-1 and LD-2). Linear combination fit of the iron extended X-ray fine structure spectrum (EXAFS) show that 3 samples from the Nu-Salween River contain 20% ferrihydrite and 10% goethite without any hematite being detected but 2 samples from the Lantsang-Mekong River contain <10% ferrihydrite, 20% goethite and with 30–60% of hematite. Concentrations of reductively leached As and Fe are correlated (Pearson correlation coefficient 0.673), with an average value of extracted As being 1.7 ± 0.6 mg/kg (n = 8) and 4.3 ± 2.0 mg/kg (n = 3) for the Nu-Salween and Lantsang-Mekong river, respectively. Parameters from the Langmuir isotherm fit to sorption experiments of As(III) and As(V) onto three river sediment samples were used to estimate “sorbed” As concentrations in river sediment in equilibrium with the average river water As concentrations. The “sorbed” As concentrations were 0.8 mg/kg and 2.8 mg/kg for the Nu-Salween and Lantsang-Mekong drainage, respectively. Taken together, the data suggest that this pool of “sorbed” As in river sand, likely to have a geothermal As component, remains largely particle-bound in the oxic and circumneutral riverine environment during transport; it is subject to mobilization once buried in the floodplain areas down gradient.

1. Introduction

Arsenic (As) has been known for its ubiquitous presence in the Earth's crust, with an upper crustal abundance of 5.7 mg/kg (Hu and Gao, 2008), recently revised from an earlier estimate of 4.8 mg/kg (Rudnick and Gao, 2003). This seemly minute amount of geogenic As has resulted in elevated levels of As in groundwater primarily under reducing conditions (Smedley and Kinniburgh,

* Corresponding author. Queens College, City University of New York, Flushing, NY 11367, United States.
** Corresponding author. Institute of Geochemistry, Chinese Academy of Sciences, Guiyang 550002, China.
E-mail addresses: lishehong@vip.gyig.ac.cn (S. Li), yan.zheng@qc.cuny.edu, yzheng@ldeo.columbia.edu (Y. Zheng).

http://dx.doi.org/10.1016/j.apgeochem.2016.04.006
0883-2927/

2002) impacting human health in many countries (Ravenscroft et al., 2009). The exposed population is the largest in Bangladesh (Flanagan et al., 2012); together with India and several countries of South and Southeast Asia, it has been estimated that >100 million people are at risk of drinking water with As concentrations above the guideline value of 10 μg/L recommended by the World Health Organization (WHO) (Chakraborti et al., 2002; Mukherjee et al., 2006). The major rivers that transported and deposited the sediment from which the As-rich groundwater is drawn in these affected countries include the Indus (BGS, 2001), Ganges (Chakraborti et al., 2003), Brahmaputra (Zheng et al., 2004), Meghna (Jung et al., 2012), Irrawaddy (van Geen et al., 2014) and Mekong (Berg et al., 2007). Although these rivers originate from the Tibetan Plateau, little is known regarding whether there is any regional geochemical anomaly of As in the Tibetan Plateau's upper crust, and if so, how it may have contributed to this wide spread groundwater As problem in these drainage basins. Several authors have proposed that the tectonic setting of the Tibetan Plateau lends itself to enrichment of As (Guillot and Charlet, 2007; Nordstrom, 2012; Saunders et al., 2005; Stanger, 2005; Zheng, 2007). Thus investigation of geochemical processes responsible for As cycling in geological materials in the headwater region of the Tibetan Plateau is a crucial first step toward understanding the role of tectonics in groundwater As occurrence in the down gradient areas.

Evidence is emerging for As enrichment in geological material in Tibetan Plateau. Concentrations of As in soil samples (N = 406) from a regional survey of all 205 representative pedons in the Tibetan Plateau averaged about 20 mg/kg for soils derived from sandstone, shale, limestone, glacial deposits, alluvial sediments and lake deposits with a lower average value of 14.7 mg/kg for soils derived from igneous rocks (Zhang et al., 2002). Compared to these Tibetan soils, soils (n = 73) and stream sediment (n = 77) from Singe Tsangpo (upstream of the Indus River) and Yarlung Tsangpo Rivers (upstream of the Brahmaputra River) have recently been reported to contain even more As, averaging 43.6 mg/kg, 30.1 mg/kg for soils and 32.5 mg/kg, 24.6 mg/kg for river sediments, respectively (Li et al., 2013). Li et al. (2013) suggests that these even higher average values of As in geological material along the Singe-Tsangpo (Indus) to Yarlung-Tsangpo (Brahmaputra) Suture Zone are probably influenced by superlative enrichment of As in Tibetan geothermal water. A study of 400 geothermal water samples collected between 1973 and 1976 immediately after eruptions of geyser reported a seemingly improbable maximum value of 125,000 μg/L As, although neither the location of the hot spring nor the analytical method were provided (Zhang et al., 1982). The same study also notes high-values of a suit of volatile elements found along both sides of Yarlung-Tsangpo River. Later studies confirm abundant hydrothermal activities with over 600 hot springs identified in the Suture Zone (Zhao et al., 2002; Zhou and Qin, 1991). At local spatial scale, discharge of water with 5700 μg/L As from Yangbajing geothermal power plant (Guo et al., 2007, 2008, 2009) has resulted in elevated As in downstream water (>20 μg/L). At regional spatial scale, elevated As in Singe-Tsangpo (average As = 58.4 μg/L) and Yarlung-Tsangpo river (average As = 10.8 μg/L) water can be found 350 and 830 km from the head water downstream (Li et al., 2013).

Simultaneous river water and stream sediment As enrichment in the Indus–Yarlung Tsangpo drainages suggest sorption of geothermal sourced As as a plausible mechanism for its removal from surface water environment. Although a few studies have investigated rapid oxidation of geothermal As(III) (Gihring and Banfield, 2001; Gihring et al., 2001; Nordstrom et al., 2005; Planer-Friedrich et al., 2007, 2009; Wilkie and Hering, 1998) followed by sorption to hot spring deposits and the associated Fe-mineralogy (Inskeep et al., 2004; Mitsunobu et al., 2013), the sorption phases for As in the river sediments further downstream have not been evaluated. Numerous studies have evaluated As sorption onto synthetic and natural minerals (Dixit and Hering, 2003, 2006; Waychunas et al., 1993) and to soil (Goldberg, 1986, 2002; Zhang and Selim, 2005). Recent studies suggest that characterization of As speciation and the mineral phases in aquifer sediment using synchrotron X-ray Absorption Spectroscopy (Kocar et al., 2006; O'Day et al., 2004) combined with sorption experiment (Jung et al., 2012) can provide molecular level information of the sorption process to better understand the mobility of this sorbed As in the environment.

This study investigates the sorption process governing the partitioning of As between river water and sediment in drainage basins influenced by geothermal As input. The three rivers area of Nu(Salween)-Lantsang(Mekong)-Jinsha(Yangtze) flowing nearly in parallel to each other from north to south along the eastern edge of the Tibetan Plateau is chosen (Fig. 1). In addition to documented hydrothermal activities in this tectonically active region (Wang et al., 1990; Xu et al., 1997), floodplains in downstream sections of the Nu(Salween)-Lantsang(Mekong)-Jinsha(Yangtze) have elevated groundwater As occurrence (Berg et al., 2007; Duan et al., 2015). River and hot spring water, and river sediment and hot spring deposit samples were collected in July of 2012 and analyzed in the field and in the laboratory later to determine chemical and mineralogical compositions including selectively leached and bulk As concentrations. Sorption experiments of 2 stream sediment sample from the Nu-Salween and 1 stream sediment sample from the Lantsang-Mekong River were conducted to allow determination of partitioning coefficient of As between aqueous and solid phases. These sediment samples and two hot spring deposit samples, one each from the Nu-Salween and the Lantsang-Mekong drainage, were subject to X-ray Absorption Spectroscopy analysis for As speciation and Fe mineralogy to illuminate phases responsible for As sorption. The implication of the results on mobility of the sorbed As in stream sediment and cycling of As is discussed.

2. Materials and methods

2.1. Geological setting of the three rivers area

The three rivers area is composed of several blocks including the Lhasa Block, Qamdo-Simao Block and Songpan Garze Block which were originated in the Devonian to Late Triassic period (Hou et al., 2003; Noh et al., 2009; Wang and Burchfiel, 2000). The lithology has been divided to six parts: (1) Carbonate rocks such as limestone, chalk, dolomitic limestone and dolomite; (2) Complex lithology including sedimentary, volcano-sedimentary and volcanic rocks with some metamorphic and plutonic rocks; (3) Plutonic acidic rocks such as granite, granodiorite, quartz-diorite, and diorite; (4) Precambrian basement having medium to highly metamorphic and predominantly granodioritic-granitic character; (5) Mixed sedimentary rocks, typically with 30–70% carbonate; and (6) Silicic-clastic rocks with less than 10% carbonate consisting of clay, silt-stone, and mudstone.

The study area lies in the western part of Yunnan Province close to the collision zone with complex geological structure. As the result of recent tectonic events, geothermal activities are abundant. In total, more than 660 geothermal spring fields exist in western Yunnan, 30 of which are high-temperature hydrothermal systems with reservoir temperatures above 150 °C (Liao et al., 1986). For the three rivers study area, there are 193, 167 and 77 geothermal spring fields along the Tengchong-Gaoligongshan belt, the Changning-Lantsang-Mekong belt and east of the Jinsha-Yangtze River Fault in Northern Yunnan, respectively.

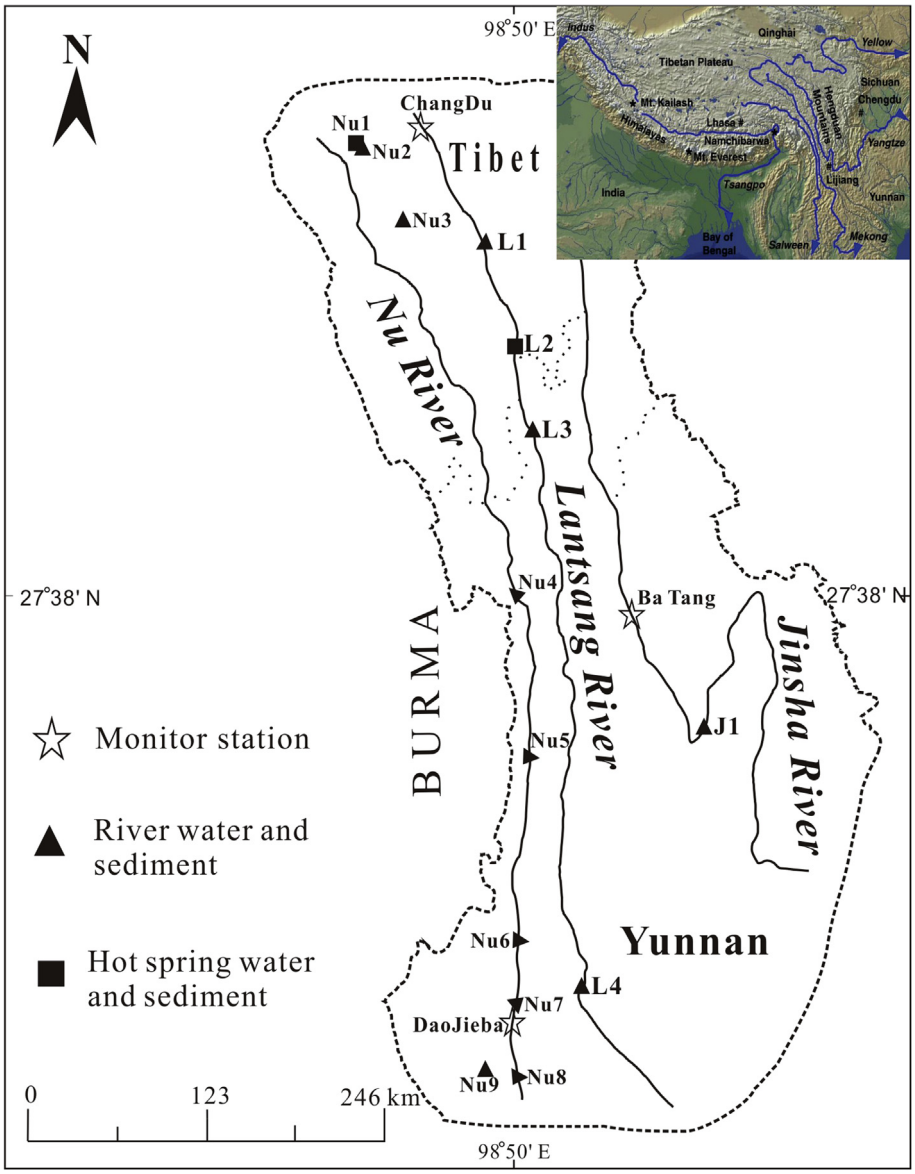

Fig. 1. Locations of river (triangle) and hot spring (square) water and sediment samples from Nu-Salween, Lantsang-Mekong, and Jinsha-Yangtze rivers in the three rivers study area located in Yunnan province of southwestern China. Star symbols represent river hydrolic monitoring stations: BaTang, ChangDu and DaoJieba.

2.2. Sample collection

Samples were collected within 97°13′ 40.5″E to 100°19′ 19.8″E and 24.8713°N to 30°10′ 13.2″N (Fig. 1) between July 1st and 17th in 2012 at 58 locations chosen to provide roughly even spatial coverage along the 694 km, 838 km and 702 km length of the Nu-Salween, Lantsang-Mekong and Jinsha-Yangtze Rivers, respectively. Sample ID consisted of the abbreviation of the name of the river, followed by the type of samples with W indicating water sample and D indicating river sediment or hot spring deposit.

As each sampling target site was approaching, the sampling point was chosen primarily based on ease of access within several kms of a target site. Hot springs within driving distance of river sampling locations were also sampled. Two aliquots of water samples were filtered through 0.45 μm membrane syringe filter into 50 ml acid-washed for cation and As analysis or 50 ml water-washed polyethylene bottle for anion analysis. Samples for cation and As analysis were acidified with concentrated HCl (trace metal grade, >37%) to pH to 1. In the field, temperature, conductivity, oxidation-reduction potential and alkalinity data were obtained for water using HACH sensION 156 and Aquamerck's alkalinity test kit. All water samples were stored in polyethylene bottles and kept at 4 °C. Sediment samples were grabbed from river bed and were stored wet in zip-lock bags and then Mylar bags and transported to the laboratory in 7 days and kept at 4 °C.

2.3. Laboratory analysis

2.3.1. Chemical analysis of water

At the State Key Laboratory of Environmental Geochemistry (SKLEG), Institute of Geochemistry of Chinese Academy of Sciences, concentrations of As in water samples were measured by hydride generation-atomic fluorescence spectroscopy method (AFS-920) following our previously established procedure (Qin et al., 2010). In brief, a mixed solution of ascorbic acid, thiourea and HCl were added into samples to reduce the As(V) to As(III) species for 25 min.

Then the arsenic concentrations in samples were measured by HG-AFS according to calibration curve established through dilution of arsenic standard solution GSB04-1714 (As(V) = 1000 mg/L) from the Certified Reference Material Center, China. Each sample was subjected to triplicate analyses to ensure a precision of <5%. Major cations were measured by the inductively coupled plasma-optical emission spectroscopy (ICP-OES, Wasst-mpx, Agilent). Anions were measured by ion chromatography(IC, DIONEX ICS-90) following U.S. EPA method 300.0.

2.3.2. Bulk mineralogical and chemical analysis of solids

Aliquots of sediments and hot spring deposits were first air-dried and powdered. A handheld X-ray fluorescence spectrometer (XRF, INNOV-X ALPHA-6500R) was used to measure the major elements and in duplicates for each sample. Bulk mineralogy of the air dried sediment or hot spring deposit samples were obtained through X-ray diffraction analysis (XRD, D/Max-2200) also at SKLEG following a routine procedure (Meng et al., 2014).

For As analysis, acid digestion using high-pressure canisters was performed. Briefly, 3 ml concentrated HNO_3 (trace metal grade) and 1 mL concentrated $HClO_4$ (trace metal grade) were added to 0.0500 ± 0.0003 g of solids in Teflon bottles, placed in oven at 160 °C for 24 h or longer until the digest became clear. The digested samples were then heated on a hot plate to nearly dryness and re-dissolved with 1% HNO_3 for analysis by HG-AFS using the same procedure for water As analysis above. For quality control, two blanks and two standard soils G14 (As = 6.5 ± 1.3 mg/kg) and G16 (As = 18 ± 2 mg/kg) were included with each batch of digestion. The results were comparable with reported values of As in standard soils within 90%–110%.

Reductive leaching was performed to evaluate the As adsorbed onto ferromanganesian oxides or carbonate minerals following a well-established procedure (Chester and Hughes, 1967). Five mL of 1 M hydroxyl amine hydrochloride in 25% acetic acid were added to a centrifuge tube containing about 0.5 g of solids to be shaken at room temperature for 4 h on a shaker. The samples were then centrifuged at 3500 rpm for 10 min. The supernatants were analyzed for As by HG-AFS similarly as above.

2.3.3. Batch sorption experiment and Langmuir isotherm

Sorption experiments began approximately 60 days after sample collection to evaluate As partitioning between river water and sediments. The sediment samples were kept wet and refrigerated at 4 °C, so were the filtered river water samples collected from the same location. Three river sediments NuD-6, NuD-4 and LD-1 were chosen for sorption experiment because they show most reductively leachable As for each river. Standard stock solutions of 1000 mg/L As(III) and 1000 mg/L As(V) were freshly prepared by dissolving $NaAsO_2$ (Sigma, >99%) and Na_2HAsO_4 (Sigma, 99.995%). Appropriate amount of solutions were added to approximately 3.0000 ± 0.0003 g of sediments suspended in 20 ml of river water in a 50 ml centrifuge tube (Sinopharm Chemical Reagent, 50 mL) to result in an initial spiked As(III) or As(V) concentration of 0 mg/L, 1 mg/L, 2 mg/L, 4 mg/L, 5 mg/L to 10 mg/L. The tubes with a screw top were sealed with Parafilm® and left on a shaker in dark for seven days. The final pH of the solutions ranged from 6.5 to 8.0, and did not change significantly from the initial pH. After seven days, the tubes were centrifuged under 4000 rpm, the supernatants were then filtered through 0.45 μm membrane for As analysis by HG-AFS as described above. Three sediment samples with the highest amount of As spike in each of the sorption experiment sequence were subjected to X-ray Absorption Spectroscopy analysis (see below) after the supernatant was removed but kept stored wet and refrigerated below 4 °C.

Results of adsorption experiment were fitted to Langmuir sorption isotherms to obtain the binding coefficient (K, L/mg) and sorption capacity (M, mg/kg) with Origin 8.0.

2.3.4. Synchrotron X-ray Absorption Spectroscopy

X-ray Fine Structure (XAFS) spectroscopy was used to assess the chemical bonding environment of Fe and As in sediments. These measurements were conducted on beam line 1W1B at Beijing Synchrotron Radiation Facility (BSRF) in 2012 and 2013. The sorption energy ranged from −200 to 1000 eV, and the K-edge of As and Fe was 11,868 eV and 7112 eV, respectively.

Arsenic spectra were compared with common standard compounds with a variety of redox states, including arsenopyrite (FeAsS), sodium arsenite ($NaAsO_2$), orpiment (As_2S_3), realgar (AsS), sodium arsenate heptahydratearsenate ($Na_2HAsO_4{\cdot}6H_2O$) and scorodite ($FeAsO_4{\cdot}2H_2O$). The $NaAsO_2$ and $Na_2HAsO_4{\cdot}6H_2O$ were purchased from Sigma–Aldrich. The other As standards were obtained from Certified Reference Material Center, China, with purity confirmed by XRD analysis. These standard compounds were powdered and pasted on Kapton tapes, with spectra collected in transmission mode. Sample thicknesses were determined based on the quantity of mineral needed to achieve a 1 μx absorption edge (about 10–20 mg over an area of a few cm^2). Except for those crystalline As-containing standards, sorption standards of As were prepared following the procedure below: Adding As(V) to a variety of common mineral compounds acting as adsorbents (2 g/L suspension density) to reach an initial spiked As concentration of 100 mg/kg. The pH of these solutions was then adjusted to be between 7.0 and 7.5. The following model compounds were included based on the results of bulk sediments XRD and XRF analysis: goethite, ferrihydrite, hematite, pyrolusite, bauxite, montmorillonite, and kaolinite. Goethite and ferrihydrite were synthesized according to the modified Schwertmann method (Cornell and Schwertmann, 2004), with purity and structure confirmed by XRD. Other model compounds were obtained from the Certified Reference Material Center, China. Due to the much lower As content sorbed to these model compounds than As-containing minerals, fluorescence mode with Lytle detector was utilized for collection of the spectra. River sediment with or without As spike and hot spring deposit samples were also analyzed in fluorescence mode. To correct for energy drift, scorodite ($FeAsO_4{\cdot}2H_2O$) spectrum was collected in parallel in all spectra data collection and opened as reference channel to correct energy shift.

To evaluate Fe mineralogy in sediments, Fe K-edge XAFS spectra of samples were compared with the spectra of a number of common Fe standards. The spectra of hematite (Fe_2O_3), ferrihydrite ($Fe(OH)_3$), crystalline goethite (α-FeOOH), siderite ($FeCO_3$), pyrite (FeS_2) were collected in transmission mode. Ferrihydrite and goethite were synthesized as described above. The other compounds were obtained from the Certified Reference Material Center, China. The spectra of Fe-bearing silicates (biotite, hornblende and Fe-rich illite) were collected in fluorescence mode at the Sanford Synchrotron Radiation Laboratory (SSRL) on beam line 11-2 using a 32 element Fe detector. Natural biotite, hornblende and Fe-rich illite were obtained from Ward's Scientific, and were ground to fine powder with an agate mortar-and-pestle before use. A small quantity (a few mg) of powder was mounted as a thin film on Kapton to ensure that the mineral grains were not impacted by self-absorption. The monochromator crystal used was Si (220) with phi angle of 0°. Soller slits and 5 μx Mn Soller slits were installed to minimize the effects of scattered primary radiation. The beam was detuned as needed to reject higher-order harmonic frequencies and prevent detector saturation. Scans were calibrated to Fe K-edge of Fe metal (7112.0 eV) using the transmission spectrum of a metal foil placed between the second and third ionization chambers.

XANES and EXAFS spectra were analyzed using the ATHENA

program in IFEFFIT package according to a recommended standard procedure (Ravel and Newville, 2005). The background was first subtracted by a linear equation that was fitted to the region below the absorption edge and a polynomial function of degree 2 that was fitted to the EXAFS region. Then the spectra were normalized by the cubic spline method. The normalized data were then used for a linear combination fit (LCF) after the well energy (E_0) calibration and aligned. The As XANES linear combination fit was done for the energy range from −20 to 35 eV. For linear combination fit in the K space for both Fe and As, all standards and samples were also pre-processed and then fits were done at the K range from 2 to 12 $Å^{-1}$ and 2 to 13 $Å^{-1}$ for As and Fe respectively. LCF methods yielded fit qualities as estimated with χ^2 of $\leq$1, and estimated fit errors of <5% for each mineral reference compound.

3. Results

3.1. Chemistry of river and hot spring water

We report water chemistry data from locations where river sediment was subjected to As sorption experiments out of a total 41 water samples collected. Water samples from the Lantsang-Mekong River (n = 2) and the Nu-Salween River (n = 1) are of Ca−HCO3 type with slightly alkaline pH (Table 1), consistent with earlier reports that attributed this to weathering of carbonate (Huang et al., 2009). Concentrations of As are <3 μg/L (Table 1). We also report water chemistry data of two hot springs out of a total of 11 sites where the hot spring deposits have been subject to XAFS analysis. One of the hot spring samples with very high NaCl is located in Yanjing, Tibet (hence the name Yanjing or Salt Well) and has 785 μg/L of As (Table 1). Hot spring from Zuogong, Tibet is Na−HCO3 type, is much fresher, and has 399 μg/L of As (Table 1). Enrichment of As in geothermal waters has been recognized around the world (Webster and Nordstrom, 2003), including the Tibetan plateau (Guo et al., 2007).

3.2. Mineralogy of river sediments and hot spring deposits

The major minerals, defined as 9% and above in percentage (Table 2), are different for the three river sediment samples. LD-1 is silty sand with mostly two minerals: 74% quartz and 10% calcite (Table 2). NuD-4 is fine sand consisted of two minerals: 69% of quartz and 10% plagioclase (Table 2). NuD-6 is coarse sand with a more varied composition: 37% quartz, 25% illite, 12% plagioclase and 9% calcite (Table 2). For the two hot spring sediments, LD-2 is consisted of 65% quartz and 11% illite. But NuD-1 is made of 82% of calcite.

The clay minerals including montmorillonite, illite and kaolinite are present in the river sediment and hot spring deposit samples in varying quantities, although only illite is present in all samples (Table 2). The coarse sand sample NuD-6 also has the highest percentages of illite and kaolinite. The upstream Nu-Salween river sediment NuD-4 contains less illite and kaolinite than NuD-6 downstream. The sampling distance (Fig. 1) between NuD-4 and NuD-6 is about 240 km and the river flow is highly variable thus there is considerable sorting of river sediments. LD-1 has the least amount of clay minerals.

The linear combination fit of XAS spectra using standard iron minerals revealed presence of iron oxides/hydroxides, iron silicates, iron carbonate and sulfide (Table 3 and Fig. 2). Although ferrihydrite, hematite and goethite were identified in variable percentages in river sediments and hot spring deposits (Table 3), we interpret the results as reflecting ubiquitous presence of secondary ferric oxyhydroxide mineral phases. The oxidation state of iron in river sediments is dominantly Fe(III) but the Fe(II) peak is also evident in XANES (Fig. 3d). Finally, >10% of iron sulfide (FeS_2) minerals was identified in NuD-1 hot spring deposit but not in LD-2 hot spring deposit (Table 3).

3.3. Bulk and reductively leached concentrations of arsenic in river sediments and hot spring deposits

Both the river sediment and hot spring deposits are enriched in As compared to the upper crustal As abundance. Two hot spring deposits contained nearly 10 times as much total As as the river sediments (average 17.3 ± 6.5 mg/kg, n = 12, Table 4). Sediment samples from the Lantsang-Mekong River showed the highest average As concentration of 26 mg/kg (n = 3), compared to an average value of 16 mg/kg for the Nu-Salween River (n = 8) or 18 mg/kg for the Jinsha-Yangtze River (n = 1, Table 4). Due to small sample size, there is no statistical significance in these differences. The abundance of As was recently estimated to be 5.7 mg/kg, 3.1 mg/kg, 0.2 mg/kg for the upper, middle and lower crusts, respectively. It is worth noting that river sediment samples analyzed here are mostly sand (Table 4), which usually contains less As than clay or silt. A survey of As in stream sediments of the three rivers area in eastern Tibet for ore prospecting found a regional average value for As of 19.5 mg/kg, with prominent local anomalies associated with elements including W, Sn, Bi, and Sb thought be derived from hydrothermal fluids (Du and Xu, 2001).

The percentages of reductively leached As in hot spring deposits (60%, 48%) are higher than those of the river sediments (7%–23%). On average, 12%, 16%, and 23% of As were reductively extracted from

Table 1
Chemical compositions of water.

Sample	Location	N	E	H(m)	pH	T °C	As μg/L	Ca^{2+} mg/L	Na^{+} mg/L	K^{+} mg/L	Mg^{2+} mg/L	Cations mEq/L	HCO_3 mg/L	F^{-} mg/L	Cl^{-} mg/L	NO_3^{-} mg/L	SO_4^{2} mg/L	Anions mEq/L
Lantsang river																		
LW1	Rumei Town, Tibet	29°37′ 04.6″	98°21′ 07.5″	2765	8.2	15	2.6	39.3	9.7	1.3	11.9	3.4	25.2	0.1	8.3	2.1	52.1	1.8
Nu river																		
NW-4	Gongshan Country, Yunna	27.637°	98.7308°	1375	8.1	17	1.1	28.0	3.5	0.8	10.5	2.5	97.6	0.1	0.6	1.0	43.8	2.6
NW-6	Liuku, Yunan	25.683°	98.87°	762	8.1	19	0.2	23.0	2.8	0.8	8.3	2.0	54.9	0.0	0.5	0.8	37.7	1.7
Hot spring																		
LW-2	Yanjing Town, Tibet	29°02′ 52.7″	98°35′ 29.3″	2305	6.9	28	785.0	974.6	10091.0	760.6	155.9	522.1	665.1	0.0	17642.6	6.1	581.5	520.1
NW-1	Zuogong Country, Tibet	30°10′ 13.2″	97°24′ 58.8″	4016	6.9	Hot	398.7	48.7	501.1	41.9	9.7	26.4	1208.2	6.2	68.4	0.4	468.8	31.5

Table 2
Mineralogy of river and hot spring deposits.

Samples	Quarts	Plagioclase	Calcite	Dolomite	Iron	Montmorillonite	Illite	Kaolinite
River sediments								
LD-1	73.69	5.65	10.25	1.62	3.05	n.d [a]	2.62	3.11
NuD-4	68.80	10.35	7.11	5.06	0.85	n.d [a]	5.06	2.77
NuD-6	37.04	12.45	9.18	3.25	n.d [a]	1.15	24.62	7.45
Hot spring deposits								
LD-2	65.13	4.82	3.06	9.13	4.16	2.46	11.24	n.d [a]
NuD-1	11.66	0.63	82.02	n.d [a]	0.81	1.24	3.58	0.87

[a] Not detected.

Table 3
Results of linear combination fit of Fe mineralogy in sediments.

Sample	Iron oxides and hydroxides			Fe–Silicates			Ferrous	Iron sulfide	Chi^2 [a]	Red-Chi^2 [a]
	Ferrihydrite (%)	Hematite (%)	Goethite (%)	Hornblende (%)	Illite (%)	Biotite (%)	$FeCO_3$ (%)	FeS_2 (%)		
River sediments										
LD-1	10 ± 3	28 ± 2	16 ± 3	30 ± 6	n.d	12 ± 2	4 ± 2	n.d	60	0.28
NuD-4	23 ± 1	n.d	6 ± 2	30 ± 3	n.d	21 ± 2	17 ± 3	3 ± 2	42	0.19
NuD-6	19 ± 2	n.d	4 ± 4	32 ± 2	4 ± 3	20 ± 2	18 ± 2	2 ± 1	41	0.18
Hot spring deposits										
LD-2	3 ± 4	60 ± 2	19 ± 2	12 ± 3	5 ± 2	n.d	2 ± 4	n.d	49	0.23
NuD-1	21 ± 5	n.d	17 ± 2	22 ± 3	5 ± 2	18 ± 2	n.d	17 ± 1	53	0.25

[a] Chi^2 and Red-Chi^2 are estimated depending on the uncertainty in data. Smaller value represents better fit.

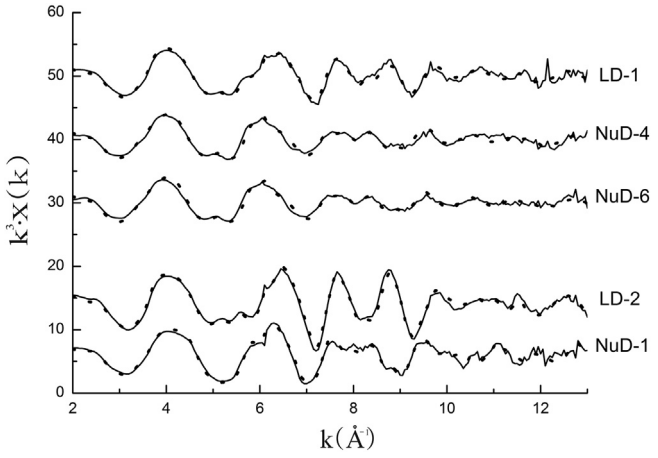

Fig. 2. Linear combination fit for Fe mineralogy in sediments based on EXAFS spectra of standard iron minerals (ferrihydrite, hematite, goethite, siderite, pyrite, hornblende, illite and biotite). The solid lines represent data and the dashed lines are fit results (see Table 3).

Nu-Salween, Lantsang-Mekong and Jinsha-Yangtze river sediments. Concentrations of extractable As and Fe in river sediments are correlated with a Pearson correlation coefficient of 0.673 ($\alpha < 0.05$, Table 4), although there were no correlations between extractable As and Mn, or between As and Al (Table 4). The correlation between reductively leached As and Fe suggests that Fe oxides/hydroxides were carrier phases for As. That reductive leaching released As also suggests that this As may be mobile under reducing conditions. Although sequential extraction has been used to determine operationally defined fractions (Mulligan and Yong, 2004; Tessier et al., 1979), the correlation and association observed in extracted elements can benefit from further mechanistic investigation. Therefore, XAS data obtained on a small number of samples are reported below to shed further light on As and Fe association in these sediments.

3.4. Arsenic XANES of river sediments and hot spring deposits

The absorption edge energies of the normalized XANES of arsenopyrite (FeAsS), realgar (AsS), orpiment (As_2S_3), arsenite ($NaAsO_2$), disodium orthoarsenate heptahydrate arsenate (Na_2HAsO_4) and scorodite ($FeAsO_4$) were 11866.8, 11868.1, 11868.8, 11870.3, 11873.3and 11873.4 eV, respectively (Fig. 3a), consistent with previous studies (Foster et al., 1998; Han et al., 2011). When the As oxidation state increases from 0 to 5 in the standard compounds, the absorption edge shifts toward higher energy level (Fig. 3a).

Two absorption peaks with energy at 11868.0 and 11874.3eVwere evident in the XANES spectra of the river and hot spring sediments (Fig. 3c). These peaks suggest a mixed As oxidation states in these sediments. Indeed, both river sediment and hot spring deposits achieved the best fist by a combination of arsenopyrite or AsS and scorodite (Table 5). We interpret the fit reflect the presence of As–Fe-sulfide mineral as well as presence of As(V)-oxyanion that may have formed bonds with another Fe phase, i.e. sorbed AsO_4 instead of a scorodite phase *per se*. Two river sediments and one hot spring deposit samples collected from the Nu-Salween River has about a third of As–Fe-sulfide mineral and two thirds of AsO_4 phases (Table 5). The Lantsang-Mekong river sediment and hot spring deposits are dominated by AsO_4 or As(V) species (Table 5). Because the bulk mineralogy of the sediment and hot spring deposit samples varied a great deal (Table 2), we do not know whether the difference in As speciation between the Nu-Salween and Lantsang-Mekong river drainages is due to geological source material difference or not. We stress that it is very likely that arsenian pyrite ($FeAs_xS_y$) instead of arsenopyrite, substitution of arsenic into the crystal structure of pyrite, are present and are not "detected" because the limitation of linear combination fit (Nordstrom, 2002).

3.5. Arsenic sorption isotherms

Results of the paired As(III) and As(V) batch sorption experiments of three river sediment samples fitted well to Langmuir sorption isotherms with high correlation coefficients ($R^2 > 0.95$

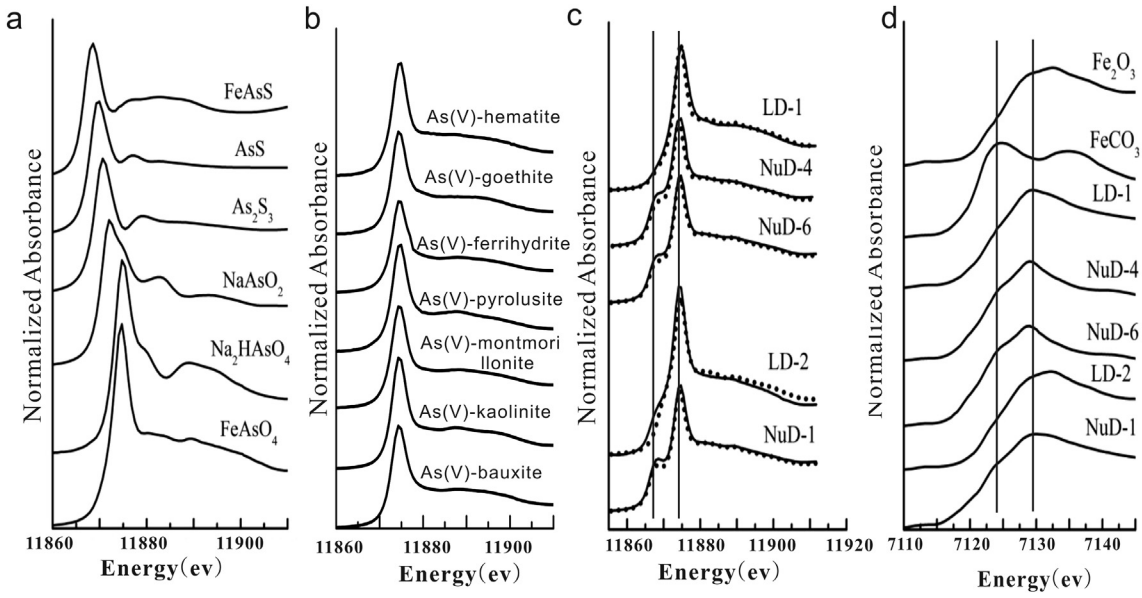

Fig. 3. Normalized XANES for a) standard As minerals such as FeAsS, As_4S_4, $NaAsO_2$, Na_2HAsO_4 and $FeAsO_4$(V); b) As(V) adsorbed onto model compounds including hematite, goethite, ferrihydrite, pyrolusite, montmorillonite, kaolinite and bauxite; c) Linear combination fit of river sediment (LD-1, NuD-4, NuD-6) and hot spring deposits (LD-2, NuD-1) using standards in Fig. 3a (see Table 5 for fitting results); d) Fe in river and hot spring deposits and standard Fe minerals such as $FeCO_3$ and Fe_2O_3.

Table 4
Arsenic concentration in river and hot spring sediments by total dissolution and by hydroxylamine hydrochloride extraction.

Sediments number	Sampling site	Sample size	Total As (mg/kg)	Total Fe (mg/kg)	Total Mn (mg/kg)	Extractable As (mg/kg)	Extractable Fe (mg/kg)	Extractable Mn (mg/kg)	Extractable Al (mg/kg)
River sediments									
LD-1	YTD-27	Silty sand	30.5	24166.7	460.8	6.25	3072	292.8	214.3
LD-3	YTD-19	Fine sand	20.1	18682.3	454.8	2.35	1303	278.6	168.9
LD-4	YTD-38	Fine sand	26.2	21357.1	457.2	4.30	2860	203.7	147.5
NuD-2	YTD-34	Fine sand	15.4	33030.0	874.6	1.44	2061	315.8	223.2
NuD-3	YTD-30	Silty sand	19.9	27273.3	500.1	1.54	2201	398.7	222.2
NuD-4	YTD-46	Fine sand	17.8	22686.7	316.2	2.22	1839	344.6	250.2
NuD-5	YTD-42	Coarse sand	10.5	19292.1	483.2	1.28	2441	157.9	299.9
NuD-6	YTD-40	Coarse sand	14.6	15672.1	855.5	2.37	2453	314.2	347.9
NuD-7	YTD-47	Coarse sand	6.8	19241.9	362.7	0.50	923	146.5	352.8
NuD-8	YTD-51	Fine sand	16.2	25303.7	803.9	2.17	2432	185.7	207.9
NuD-9	YTD-52	Coarse sand	12.4	17605.5	622.5	1.92	713	116.8	377.3
JD-1	YTD-17	Fine sand	17.7	24556.9	468.3	4.10	3147	238.2	128.5
Spring deposits									
NuD-1	YTD-33	Silty sand	101.9	18856.6	441.6	61.10	9648	310.5	93.1
LD-2	YTD-23	Silty sand	263.7	26000.5	460.6	125.81	8181	363.1	186.8

Note: Ext As-Ext Fe (river sediments, n = 12): $\rho = 0.673$, $\alpha = 0.02$; Ext As-Ext Mn (river sediments, n = 12): $\rho = 0.134$, $\alpha = 0.68$.
Ext As-Ext Al(river sediments, n = 12): $\rho = -0.549$, $\alpha = 0.06$.
ρ: Pearson correlation coefficient.
α: significance level.

Table 5
XANES result of arsenic speciation in river sediments and hot spring deposits.

Samples	As(V) (%)	Arsenopyrite-like (%)	AsS (%)	R-factor[a]
River sediments				
LD-1	90 ± 1	10 ± 1	n.d[b]	0.004
NuD-4	68 ± 2	32 ± 2	n.d[b]	0.005
NuD-6	68 ± 1	32 ± 1	n.d[b]	0.002
Hot spring deposits				
LD-2	93 ± 2	n.d[b]	26 ± 2	0.005
NuD-1	65 ± 1	35 ± 1	n.d[b]	0.002

[a] The R-factor represents the relative error of the fit and data. Smaller value represents better fit.
[b] Not detected and thus not included in final fit.

Table 6). Sorption isotherms show that the coarse sand sediment NuD-6 has the lowest sorption capacity for As(III), although the sorption capacity for As(V) is only slightly lower than that of the fine sand sample NuD-4 (Table 6). Sorption isotherms are similar for As(III) and As(V) for the river sediment NuD-4 consisted of fine sand (Fig. 4a), with comparable binding coefficient (K) and sorption capacity (M) values (Table 6). Sorption isotherms of As(III) and As(V) are also similar for silty sand sample LD-1 (Table 6), although a lower sorption capacity for As(V) is observed. It has been shown that As(III) can be sorbed to a similar or greater extent than As(V) on ferrihydrite and goethite when pH is >7 (Dixit and Hering, 2003). Our sorption experiments were conducted with river

Table 6
Langmuir parameters of sorption experiment.

Samples	Parameters		
	K (L/mg)[a]	M(mg/kg)[b]	R^2
LD-1 As(III)	4.9	134.3	0.99
LD-1 As(V)	6.8	94.5	0.98
NuD-4 As(III)	6.7	77.6	0.98
NuD-4 As(V)	5.6	75.1	0.96
NuD-6 As(III)	7.9	33.7	0.97
NuD-6 As(V)	1.5	69.9	0.96

R^2 is correlation factor.
[a] K is binding coefficient.
[b] M is saturation adsorption capacity.

spectra (Fig. 4b), although a mixed As(III) and As(V) were expected due to the presence of As(III) in the unspiked samples (Fig. 2). It is likely that because the spiked As(V) is 0.5–4 times higher than the total bulk As concentration of the sediment samples, detection of As(III) is difficult. In the case of As(III) addition, only the coarse sand sediment NuD-6 showed a detectable As(III) peak but not NuD-4 or LD-1 (Fig. 4b). Having the confirmation that As(III) is observed in spiked sample provides confidence that the differences in sorption isotherm (Fig. 4a) and Langmuir parameters (Table 6) observed in NuD-6 between As(III) and As(V) is likely due to differences in the As speciation in the solution.

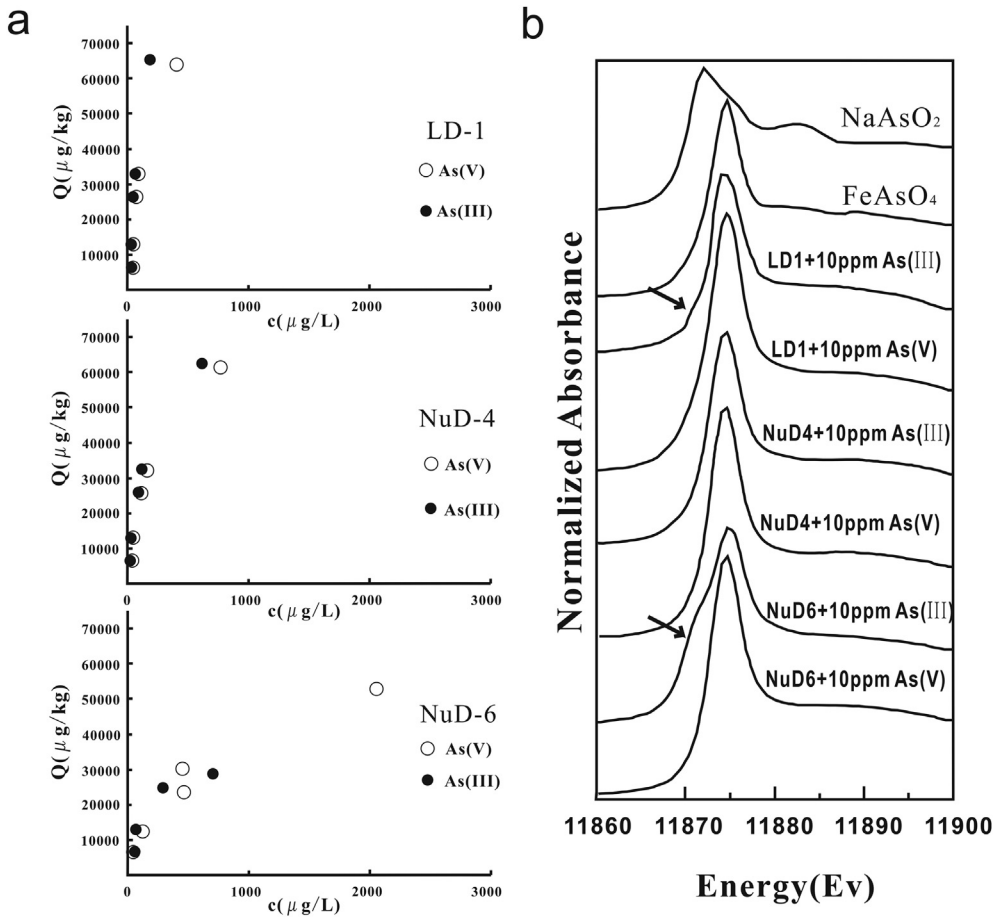

Fig. 4. a) Sorption isotherms of NuD-6, NuD-4 and LD-1 (Langmuir parameters see Table 6), with open and solid circles representing As(V) and As(III) spikes, respectively. For As(III) addition to NuD-6, the highest point (5180 μg/L aqAs and 32, 130 μg/kg sorbed As) is not shown due to x-axis scale. b) XANES of As for NuD-6, NuD-4 and LD-1 samples spiked with 10 mg/L As(V) or As(III).

water having pH value of 8 and with river sediment samples in which iron oxyhydroxide minerals have been identified (Table 3). Sorption isotherms for LD-1 is consistent with a recent study demonstrating that the relative affinity of As(V) and As(III) to iron oxyhydroxide minerals is not always in favor of As(V) because addition of Fe ions has been shown to result in higher affinity of As(III) with sediments and soils (Dousova et al., 2012).

Interpretation of the sorption isotherms nevertheless needs to consider the effects of oxidation of spiked As(III) that may have occurred over the course of the experiment. In the case of As(V) addition, all three sediment samples after As(V) addition reached sorption equilibrium displayed only As(V) peak in their XANES

3.6. Sorption phases and As interaction by XAS

Although the sorption phases consisted of Fe-, Mn- oxides/hydroxides and clay minerals have all been recognized as probable minerals for As sorption by soil and sediment (Goldberg, 2002; Manning and Martens, 1997), data suggest stronger affinity of As for secondary iron minerals in these river sediments and hot spring deposits over Mn- and Al- oxides and clay minerals. To further illuminate the interaction of As with the possible sorption phases, the XAS spectra of 100 mg/kg As adsorbed onto 7 standard minerals, including goethite, ferrihydrite, hematite, pyrolusite, bauxite, montmorillonite, and kaolinite, were obtained (Fig. 3b). These

spectra were then used for a linear combination fit to illuminate As and possible sorption phases of the EXAFS of river sediment samples. The LCF were done only to samples with the highest amount of As(V) sorbed onto, or the sediment sample with 10 mg/kg or the highest amount of As(V) spikes in the sorption experiment. Excellent fits were obtained for all (Fig. 5). Association between As and iron oxyhydroxide minerals was confirmed because all three fits identified a large percentage of such Fe secondary mineral model compounds sorbed with As (Table 7). In LD-1, interaction between As and Mn oxides was also identified (Table 7). Further, consistent with hematite determined from Fe EXAFS in LD-1 (Table 3), this LCF also finds As-hematite as being important (Table 7). In NuD-4 and NuD-6, interaction between As and clay minerals was evident (Table 7).

Applying the LCF to two hot spring deposit samples (no As addition), the most significant association is once again As with Fe secondary minerals (Table 7), with some As–MnO_2 interaction. It is worth noting the fit for NuD-1 (Fig. 5) is not as good as the fit for LD-2 as evidenced by the R factor (Table 7) possibly because we did not include an Fe carbonate sorbed As as a standard mineral and NuD-1 had 82% calcite (Table 2).

4. Discussion

4.1. Arsenic in hot spring deposits

Superlative levels of arsenic in continental geothermal water (Webster and Nordstrom, 2003) have resulted in downstream surface water arsenic enrichment in many hydrothermally active regions including Tibet (Guo et al., 2008; Li et al., 2013) but is especially well demonstrated for the Waikato River, New Zealand (McLaren and Kim, 1995; Webster-Brown and Lane, 2005; Wilson and Webster-Brown, 2009) and rivers down streams of Yellowstone, USA (McCleskey et al., 2010; Nimick et al., 1998). However, the only known case of population level human exposure to geothermal sourced riverine As is the Loa River that supplied water to the arid Atacama Desert for the Antofagasta Region in Northern Chile (Smith et al., 1998). Only a few studies investigated geochemistry of As in hot spring deposits using X-rays from synchrotron sources to shed light on its mobility. Siliceous sinter material sampled from a hydrothermal channel from Antofagasta Region in Northern Chile has been analyzed, with least-squares linear fitting of μ-XANES spectra indicating that 63% of As is arsenate sorbed on hydrous ferric oxides and 37% of As is nodular arsenide micro-mineralizations similar to loellingite ($FeAs_2$). Hot spring discharge and deposit samples taken at 0, 2, 4, 6 and 8 m from the discharge point of Sambe hot spring, Shimane, Japan not only confirm the rapid microbially driven As(III) oxidation in water (Wilkie and Hering, 1998), Fe and As K-edge XANES spectra of all deposits suggest presence of only As(V) and Fe oxyhydroxide (Mitsunobu et al., 2013). Investigation of microbial mats of an acid-sulfate-chloride hot spring at the Yellowstone National Park revealed that As-rich, poorly ordered nanocrystalline hydrous ferric oxides formed sheaths external to microbial cell walls, with bonding environment of As(V) and Fe(III) consistent with adsorption of arsenate on edge and corner positions of Fe(III)–OH octahedral (Inskeep et al., 2004). Our results add to this small body of literature on investigation of As in hot spring deposits by X-rays from synchrotron sources. Consistent with the aforementioned studies, in both the siliceous (quartz dominant) and the calcareous (calcite dominant) hot spring deposits, As speciation is dominated by As(V) that is primarily sorbed to ferrihydrite, and to a lesser extent, goethite/hematite and MnO_2.

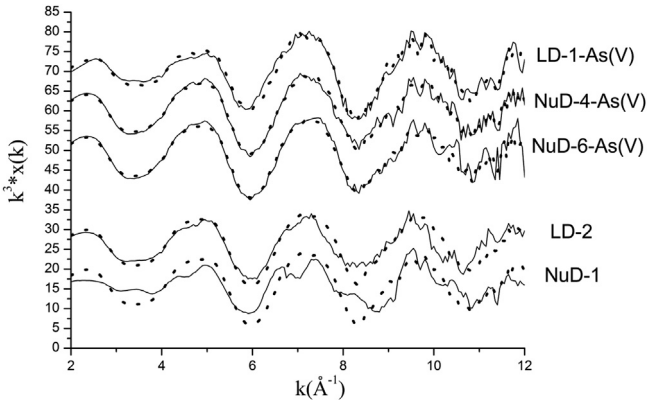

Fig. 5. EXAFS linear combination fit (see Table 7 for results) of sediments with 10 mg/L As(V) spike and two hot spring deposits modeled using EXAFS spectra of As(V) sorbed onto standard minerals (Fig. 3b). The solid lines represent data and the dashed lines are fit results.

4.2. Low mobility of arsenic in surficial environment

The understanding gained by application of synchrotron techniques to study As mobility of mine tailings and contaminated soils is used as a framework to interpret our XAS results of As in river sediments and hot spring deposits. Since late 1990s, the powerful X-rays from synchrotron sources have been used to investigate molecular-level speciation of As in environmental samples to shed light on its mobility, with many of the studies of mine tailing and contaminated soils samples often with hundreds if not thousands of mg/kg As (Brown et al., 1999; Jamieson, 2011). These studies unequivocally support the pivotal role of hydrous ferric oxides in delaying the transfer of As from contaminated surficial environment to biota (Morin and Calas, 2006) because As strongly bound in crystalline or sorbed to X-ray amorphous precipitates is generally considered to have low bioaccessibility in surficial environment. For example, EXAFS analysis of As K-edge spectra of a variety of mine tailing samples has found that As(V) (arsenate) is adsorbed to the ferrihydrite through an inner-sphere bidentate linkage. The tailing samples examined include U mine tailings in northern Saskatchewan, Canada (Essilfie-Dughan et al., 2012, 2013; Moldovan et al., 2003), Cu–W–As mine tailings in SW Finland (Parviainen et al., 2012), and Au mine tailings in Nova Scotia, Canada (Walker et al., 2009). Similar to mine tailings, in contaminated soil samples As was frequently found to occur in three forms: As adsorbed on iron hydroxides, scorodite ($FeAsO_4 \cdot 2H_2O$), and As(V) containing jarosite (Vodyanitskii, 2006). The strong association between As(V) with Fe(III) oxide phases has been observed in mine waste contaminated soil in Madrid Province, Spain (Gomez-Gonzalez et al., 2014), although off-site transport by leaching of scorodite during rain storms has also been observed. In the French Massif Central, soil with >1000 mg/kg As has three forms: arsenates mostly as pharmacosiderite, Fe-oxyhydroxides with As content up to 15.4 wt% and aluminosilicates (Bossy et al., 2010). Similar interaction between As and Fe is observed in soil developed over pyritic shale in the Panoche Hills on the east side of the California Coast Range: As was found to be preferentially associated with the iron oxide aggregates consisted of ferrihydrite (Strawn et al., 2002). Considering the similarities and the strong and dominant As and Fe oxyhydroxides association observed in river sediments and hot spring deposits, we suggest that As in these riverine systems influenced by geothermal As input is reasonably stable under current conditions and poses no immediate environmental health threat. The low mobility of the sorbed As further indicates that such As is transported downstream as discussed below.

Table 7
EXAFS lcf analysis for adsorption phases using adsorption model compounds.

Sample	As-iron hydroxides/oxides				As–MnO_2	As-kaoline	As-bauxite	R-factor[a]
	As-ferrihydrite	As-goethite	As-hematite	Total (%)				
Adsorption samples								
As(V)-LD1	20 ± 7	10 ± 4	40 ± 4	70	30 ± 4	n.d.	n.d.	0.07
As(V)-NuD4	48 ± 5	32 ± 3	n.d	80	n.d.	19 ± 6	n.d.	0.04
As(V)-NuD6	54 ± 6	35 ± 4	n.d.	89	n.d.	15 ± 5	n.d.	0.07
Hot spring deposits								
LD-2	74 ± 15	10 ± 5	n.d.	84	13 ± 5	n.d	3 ± 8	0.22
NuD-1	66 ± 10	14 ± 7	4 ± 16	84	15 ± 8	n.d	n.d	0.65

[a] The R-factor represents the relative error of the fit and data. Smaller value represents better fit.

4.3. Fluxes of As transported downstream

The fluxes of arsenic transported downstream by the three rivers were estimated by summing the flux of As transported by water (F_{aqAs}) and by the sediment, considering only the "sorbed" fraction of As (F_{sorbAs}):

$$F_{As} = F_{aqAs} + F_{sorbAs} \quad (1)$$

To estimate the flux of As transported by water, annual discharge (D) data were obtained from monitor stations at DaoJieba for the Nu-Salween River (Liu and He, 2013), ChangDu for the Lantsang-Mekong River (He, 1995), BaTang for the Jinsha-Yangtze River (Pan, 1999) and multiplied by the respective average river water As concentrations (C_{aqAs}) obtained in this study:

$$F_{aqAs} = D^{*}C_{aqAs} \quad (2)$$

To estimate the flux of As transported by sediment, flux of suspended material (F_{SM}) is multiplied by the concentration of sorbed As on river sediment (Q_{sorbAs}) assuming the water and sediment is at sorption equilibrium determined through Langmuir isotherm:

$$F_{sorbAs} = F_{SM}{}^{*}Q_{sorbAs} \quad (3)$$

where

$$Q_{sorbAs} = k^{*}M^{*}C_{aqAs}/(1 + k^{*}C_{aqAs}) \quad (4)$$

The average C_{aqAs} from high to low was 4.5, 3.3 and 1.9 μg/L for the Nu-Salween, Lantsang-Mekong and Jinsha-Yangtze rivers respectively, corresponding to a low to high discharge data of these rivers from 15.2, 27.2 to 87.5 billion cubic meter per year (Table 8). While this suggests that dilution by river water plays a role in the average C_{aqAs} observed, the Nu-Salween River likely receives the most geothermal sourced As input because otherwise the riverine As level would be lower. Assuming geothermal sourced As is primarily sorbed to the sediment, the equilibrium sorbed As concentration based on the Langmuir sorption model fit (Table 6) and the average reductively leached sediment As concentrations were also the lowest for the Nu River (Table 8), again reflecting the dilution effect of the Nu-Salween river. It is interesting to note although the two methods of assessing "sorbed" As yielded different results for the Nu-Salween river and the Lantsang-Mekong river, it is worth noting that the values for the two river systems differ consistently by a factor of about 3. To summarize, the "sorbed" As on the suspended material transported downstream is estimated to range from about 1 mg/kg to 4 mg/kg.

The combined As flux transported by water and suspended material in the three rivers is estimated to be 500 tons of As per year. We do not know that this reflects entirely the geothermal input of As into these river systems because chemical weathering should still contribute to surface water As and also make it available for sorption, it is nevertheless worth noting that a geothermal As flux of Madison River downgradient from Yellowstone geothermal field has been estimated to be 3.4 g/s, equivalent to 107 tons per year (Nimick et al., 1998). Several studies have illustrated the impact of geothermal As (Zhang et al., 2008; Zhu et al., 1989) on river water As enrichment in Tibet (Guo et al., 2007, 2008, 2009; Li et al., 2013, 2014). Although much has been learned regarding hydrogeochemistry of geothermal water and river water, there is no independent assessment of geothermal As fluxes to compare our riverine As flux estimate with. We regard our estimate as plausible based on the Yellowstone study but acknowledge the need for further study in the region.

How does this geothermal sourced As flux compare to As mass accumulation rate in downgradient delta? The Salween River delta is small and not well studied, and the Yangtze River delta has a much larger catchment area making it too complex to compare. The

Table 8
Estimation of As flux of TRA.

Rivers	Monitor station	Water flux (m^3/year)	Sand flux (t/year)	Average water As (μg/L)	Average ExtAs (mg/kg)	q[d] (mg/kg)	F(As) in water(t/year)	F_q(As) adsorbed (t/year)[e]	F_e(As) adsorbed (t/year)[f]
Lantsang River (Salween river)	ChangDu	151.9×10^8 [a]	1850×10^4 [a]	4.5 ± 1.4 (n = 4)	4.30 ± 1.95 (n = 3)	2.8	68.4	51.8	79.6
Nu River (Mekong river)	DaoJieba	875.4×10^8	4061×10^4 [b]	1.9 ± 1.9 (n = 12)	1.68 ± 0.62 (n = 8)	0.8	166.3	32.5	68.2
Jinsha River (Yangtze River)	BaTang	272×10^8 [c]	1450×10^4 [c]	3.3 ± 1.8 (n = 2)	4.10 (n = 1)	–	89.8	–	59.5

[a] From (He, 1995).
[b] From (Liu and He, 2013).
[c] From (Pan, 1999).
[d] Adsorption amount of As based on Langmuir model.
[e] Flux of adsorbed As calculated from q.
[f] Flux of adsorbed As calculated from extracted As.

sediment facies and accumulation of Mekong River delta, a typical mixed tide and wave energy delta formed during the last 6 ka, has been constrained by radiocarbon dating of borehole sediments from the delta plain (Ta et al., 2002a, 2002b). The incised-valley fill consisting mainly of estuarine and bay sediments during the rise of sea level (13 ka B.P.) to the early sea-level highstand (6 ka B.P.) indicates a high accumulation rate of more than 20 m ka^{-1}. From 3 ka B.P. to present, the sediment accumulation rate was similar but became more lateral as delta prograded to the sea. The calculated sediment volume deposited during the last 3 kyr is 360 ± 90,10^9 m^3 which is equivalent to 144 ± 36 million ton yr^{-1} using a bulk density of 1.2 ± 0.1 g cm^{-3} (Ta et al., 2002b), only about 10% lower than the present sediment discharge of the Mekong River (160 million ton yr^{-1}). Based on a radiocarbon dating obtained average clay layer deposition rate of 1–3.3 m ka^{-1} over the past 6000 yr, a rate of As deposition in clay has been estimated to be 600–20,000 ton yr^{-1} using an As content of 9 mg/kg (Polizzotto et al., 2008). Because sediment accumulation has evolved from vertical accretion to lateral progradation out to sea, we believe it is better to apply the high sediment accumulation rate of ~20 m ka^{-1}, or an equivalent sediment accumulation flux of 144 ± 36 million ton yr^{-1} (Ta et al., 2002b) multiplied by an average solid-phase arsenic concentration of ~3 mg/kg in sandy aquifer sediment of the Mekong River delta (Polizzotto et al., 2008) to arrive at an As accumulation rate of the Mekong Delta aquifer of 432 ± 108 ton yr^{-1}. The flux of bulk As (average concentration 17.3 mg/k) transported by the upstream Lantsang-Mekong river (sediment flux 18.5 million ton yr^{-1}) is 315 ton yr^{-1}. The flux of "sorbed" As transported down gradient is 80 ton yr^{-1} (Table 8). It appears that As flux estimations are allowable given the sediment As accumulation rate in the Mekong River delta, and that perhaps a quarter of the As is geothermally sourced.

What is the implication of each river transporting about 50–100 tons of sorbed As downstream each year? The downstream area with elevated groundwater As tend to be relatively flat floodplains of rivers that are conducive to reducing biogeochemical environment that promotes the mobilization of such sorbed As once buried (Ravenscroft et al., 2009; Smedley and Kinniburgh, 2002). Reductive dissolution of Fe oxides/hydroxides facilitated by microbes is commonly regarded as the dominant process (Anawar et al., 2006; Campbell et al., 2006; Dhar et al., 2011; Islam et al., 2004; Smedley and Kinniburgh, 2002). Our study clearly demonstrates that As transported by river sediments is sorbed to Fe oxides/hydroxides, adding to a connection between the groundwater As enrichment downstream to source areas. However, questions remain whether sediments deposited in the downstream flood plains indeed can be traced back to these river sediments in our study, and which geologic formations in the Tibetan Plateau supplies these sediments under varied climatic conditions (Clift et al., 2008).

5. Conclusion

Abundant hydrothermal activities in the Tibetan-Plateau provide a geogenic source of "sorbed" arsenic to the rivers that supply sediment in downstream areas where groundwater As is elevated. When reductively leaching and Langmuir sorption equilibrium were both used to evaluate the concentration of this "sorbed" pool of arsenic in sediment, it was shown that it ranges from 1 to 4 mg/kg for sediment with variable grain sizes: silty sand, fine sand and coarse sand that contain an average 17 mg/kg bulk As. Using X-ray synchrotron technique, it is shown that the arsenic in hot spring and river sediment deposits are strongly sorbed to primarily secondary iron minerals such as ferrihydrite, goethite and hematite. While such sorbed As remains largely particle-bound in the oxic and neutral riverine environment during transport, it is subject to mobilization once buried in the floodplain areas down gradient. Our study illustrates an important connection from the occurrence of groundwater As to its geogenic source.

Acknowledgement

We thank Hui Wang, Pengfei An, Guangqian Yu and Kale Clauson for their valuable assistance during a three-week field excursion. We thank Benjamin Bostick and Jing Sun for sharing XAS data of Fe silicates and for discussion on data processing. Funding was provided by the National Natural Science Foundation of China (Nos. 41273146 and 41073100), the Open Fund of the Skate Key Laboratory of Environmental Geochemistry (SKLEG2013815), the Beijing Synchrotron Radiation Facility, and the U.S NSF-EAR0738888. SL received a fellowship from the Chinese Academy of Sciences to visit Lamont-Doherty Earth Observatory of Columbia University. This is LDEO contribution 7996.

References

Anawar, H.M., Akai, J., Yoshioka, T., Konohira, E., Lee, J.Y., Fukuhara, H., Alam, M.T.K., Garcia-Sanchez, A., 2006. Mobilization of arsenic in groundwater of Bangladesh: evidence from an incubation study. Environ. Geochem. Health 28, 553–565.

Berg, M., Stengel, C., Trang, P.T.K., Viet, P.H., Sampson, M.L., Leng, M., Samreth, S., Fredericks, D., 2007. Magnitude of arsenic pollution in the Mekong and Red River deltas – Cambodia and Vietnam. Sci. Total Environ. 372, 413–425.

BGS, 2001. In: Survey, B.G. (Ed.), Groundwater Quality: Pakistan. NERC.

Bossy, A., Grosbois, C., Beauchemin, S., Courtin-Nomade, A., Hendershot, W., Bril, H., 2010. Alteration of As-bearing phases in a small watershed located on a high grade arsenic-geochemical anomaly (French Massif Central). Appl. Geochem. 25, 1889–1901.

Brown, G.E., Foster, A.L., Ostergren, J.D., 1999. Mineral surfaces and bioavailability of heavy metals: a molecular-scale perspective. In: Proceedings of the National Academy of Sciences of the United States of America, vol. 96, pp. 3388–3395.

Campbell, K.M., Malasarn, D., Saltikov, C.W., Newman, D.K., Hering, J.G., 2006. Simultaneous microbial reduction of iron(III) and arsenic(V) in suspensions of hydrous ferric oxide. Environ. Sci. Technol. 40, 5950–5955.

Chakraborti, D., Mukherjee, S.C., Pati, S., Sengupta, M.K., Rahman, M.M., Chowdhury, U.K., Lodh, D., Chanda, C.R., Chakraborti, A.K., Basu, G.K., 2003. Arsenic groundwater contamination in Middle Ganga Plain, Bihar, India: a future danger? Environ. Health Perspect. 111, 1194–1201.

Chakraborti, D., Rahman, M.M., Paul, K., Chowdhury, U.K., Sengupta, M.K., Lodh, D., Chanda, C.R., Saha, K.C., Mukherjee, S.C., 2002. Arsenic calamity in the Indian subcontinent: what lessons have been learned? Talanta 58, 3–22.

Chester, R., Hughes, M.J., 1967. A chemical technique for the separation of ferromanganese minerals, carbonate minerals and adsorbed trace elements from pelagic sediments. Chem. Geol. 2, 249–262.

Clift, P.D., Giosan, L., Blusztajn, J., Campbell, I.H., Allen, C., Pringle, M., Tabrez, A.R., Danish, M., Rabbani, M.M., Alizai, A., Carter, A., Luckge, A., 2008. Holocene erosion of the Lesser Himalaya triggered by intensified summer monsoon. Geology 36, 79–82.

Cornell, R.M., Schwertmann, U., 2004. Synthesis, the Iron Oxides. Wiley-VCH Verlag GmbH & Co. KGaA, pp. 525–540.

Dhar, R.K., Zheng, Y., Saltikov, C.W., Radloff, K.A., Mailloux, B.J., Ahmed, K.M., van Geen, A., 2011. Microbes enhance mobility of arsenic in Pleistocene aquifer sand from Bangladesh. Environ. Sci. Technol. 45, 2648–2654.

Dixit, S., Hering, J.G., 2003. Comparison of arsenic(V) and arsenic(III) sorption onto iron oxides minerals: implications for arsenic mobility. Environ. Sci. Technol. 18, 4182–4189.

Dixit, S., Hering, J.G., 2006. Sorption of Fe(II) and As(III) on goethite in single- and dual-sorbate systems. Chem. Geol. 228, 6–15.

Dousova, B., Buzek, F., Rothwell, J., Krejcova, S., Lhotka, M., 2012. Adsorption behavior of arsenic relating to different natural solids: soils, stream sediments and peats. Sci. Total Environ. 433, 456–461.

Du, G.W., Xu, K.F., 2001. Geochemical characteristics of "Sanjiang" area in eastern Tibet and their ore-prospecting significance. Geophys. Geochem. Explor. 25, 425–431 (in Chinese).

Duan, Y., Gan, Y., Wang, Y., Deng, Y., Guo, X., Dong, C., 2015. Temporal variation of groundwater level and arsenic concentration at Jianghan Plain, central China. J. Geochem. Explor. 149, 106–119.

Essilfie-Dughan, J., Hendry, M.J., Warner, J., Kotzer, T., 2012. Microscale mineralogical characterization of As, Fe, and Ni in uranium mine tailings. Geochim. Cosmochim. Acta 96, 336–352.

Essilfie-Dughan, J., Hendry, M.J., Warner, J., Kotzer, T., 2013. Arsenic and iron speciation in uranium mine tailings using X-ray absorption spectroscopy. Appl. Geochem. 28, 11–18.

Flanagan, S.V., Johnston, R.J., Zheng, Y., 2012. Arsenic in tube well water in Bangladesh: health and economic impacts and implications for arsenic mitigation. Bull. World Health Organ. 90, 839–846.
Foster, A.L., Brown, G.E.J., Tingle, T.N., Parks, G.A., 1998. Quantitative arsenic speciation in mine tailings using X-ray absorption spectroscopy. Am. Mineral. 83, 553–568.
Gihring, T.M., Banfield, J.F., 2001. Arsenite oxidation and arsenate respiration by a new Thermus isolate. FEMS Microbiol. Lett. 204, 335–340.
Gihring, T.M., Druschel, G.K., McCleskey, R.B., Hamers, R.J., Banfield, J.F., 2001. Rapid arsenite oxidation by *Thermus aquaticus* and *Thermus thermophilus*: field and laboratory investigations. Environ. Sci. Technol. 35, 3857–3862.
Goldberg, S., 1986. Chemical modeling of arsenate adsorption on aluminum and iron oxide minerals. Soil Sci. Soc. Am. J. 50, 1154–1157.
Goldberg, S., 2002. Competitive adsorption of arsenate and arsenite on oxides and clay minerals contribution from the George E. Brown Jr., Salinity laboratory. Soil Sci. Soc. Am. J. 66, 413–421.
Gomez-Gonzalez, M.A., Serrano, S., Laborda, F., Garrido, F., 2014. Spread and partitioning of arsenic in soils from a mine waste site in Madrid province (Spain). Sci. Total Environ. 500, 23–33.
Guillot, S., Charlet, L., 2007. Bengal arsenic, an archive of Himalaya orogeny and paleohydrology. J. Environ. Health Part A 42, 1785–1794.
Guo, Q., Wang, Y., Liu, W., 2007. Major hydrogeochemical processes in the two reservoirs of the Yangbajing geothermal field, Tibet, China. J. Volcanol. Geotherm. Res. 166, 255–268.
Guo, Q.H., Wang, Y.X., Liu, W., 2008. B, As, and F contamination of river water due to wastewater discharge of the Yangbajing geothermal power plant, Tibet, China. Environ. Geol. 56, 197–205.
Guo, Q.H., Wang, Y.X., Liu, W., 2009. Hydrogeochemistry and environmental impact of geothermal waters from Yangyi of Tibet, China. J. Volcanol. Geotherm. Res. 180, 9–20.
Han, Y.-S., Jeong, H.Y., Demond, A.H., Hayes, K.F., 2011. X-ray absorption and photoelectron spectroscopic study of the association of As(III) with nanoparticulate FeS and FeS-coated sand. Water Res. 45, 5727–5735.
He, D., 1995. Analysis of hydrological characteristics in Lancang-Mekong river. Yunnan Geogr. Environ. Res. 7, 58–74.
Hou, Z., Wang, L., Zaw, K., Mo, X., Wang, M., Li, D., Pan, G., 2003. Post-collisional crustal extension setting and VHMS mineralization in the Jinshajiang orogenic belt, southwestern China. Ore Geol. Rev. 22, 177–199.
Hu, Z., Gao, S., 2008. Upper crustal abundances of trace elements: a revision and update. Chem. Geol. 253, 205–221.
Huang, X., Sillanpää, M., Gjessing, E.T., Vogt, R.D., 2009. Water quality in the Tibetan Plateau: major ions and trace elements in the headwaters of four major Asian rivers. Sci. Total Environ. 407, 6242–6254.
Inskeep, W.P., Macur, R.E., Harrison, G., Bostick, B.C., Fendorf, S., 2004. Biomineralization of As(V)-hydrous ferric oxyhydroxide in microbial mats of an acid-sulfate-chloride geothermal spring, Yellowstone National Park. Geochim. Cosmochim. Acta 68, 3141–3155.
Islam, F.S., Gault, A.G., Boothman, C., Polya, D.A., Charnock, J.M., Chatterjee, D., Lloyd, J.R., 2004. Role of metal-reducing bacteria in arsenic release from Bengal delta sediments. Nature 430, 68–71.
Jamieson, H.E., 2011. Geochemistry and mineralogy of solid mine waste: essential knowledge for predicting environmental impact. Elements 7, 381–386.
Jung, H.B., Bostick, B.C., Zheng, Y., 2012. Field, experimental, and modeling study of arsenic partitioning across a redox transition in a Bangladesh aquifer. Environ. Sci. Technol. 46, 1388–1395.
Kocar, B.D., Herbel, M.J., Tufano, K.J., Fendorf, S., 2006. Contrasting effects of dissimilatory iron(III) and arsenic(V) reduction on arsenic retention and transport. Environ. Sci. Technol. 40, 6715–6721.
Li, C., Kang, S., Chen, P., Zhang, Q., Mi, J., Gao, S., Sillanpää, M., 2014. Geothermal spring causes arsenic contamination in river waters of the southern Tibetan Plateau, China. Environ. Earth Sci. 71, 4143–4148.
Li, S., Wang, M., Yang, Q., Wang, H., Zhu, J., Zheng, B., Zheng, Y., 2013. Enrichment of arsenic in surface water, stream sediments and soils in Tibet. J. Geochem. Explor. 135, 104–116.
Liao, Z., Tong, W., Liu, S., Zhao, F., 1986. High-temperature hydrothermal systems in west Yunnan Province, China. Geothermics 15, 627–631.
Liu, X., He, D., 2013. Temporal and spatial distribution and its change trend of suspended sediment transport in the Nujiang River Basin. Acta Geogr. Sin. 68, 365–371.
Manning, B.A., Martens, D.A., 1997. Speciation of Arsenic (III) and Arsenic (V) in sediment extracts by High-performance liquid chromatography-hydride generation atomic absorption spectrophotometry. Environ. Sci. Technol. 31, 171–177.
McCleskey, R.B., Nordstrom, D.K., Susong, D.D., Ball, J.W., Taylor, H.E., 2010. Source and fate of inorganic solutes in the Gibbon river, Yellowstone National Park, Wyoming, USA. II. Trace element chemistry. J. Volcanol. Geotherm. Res. 196, 139–155.
McLaren, S.J., Kim, N.D., 1995. Evidence for a seasonal fluctuation of arsenic in New Zealand's longest river and the effect of treatment on concentrations in drinking water. Environ. Pollut. 90, 67–73.
Meng, Y., Gong, G., Wei, D., Xie, Y., Yin, Z., 2014. Comparative microstructure study of high strength alumina and bauxite insulator. Ceram. Int. 40, 10677–10684.
Mitsunobu, S., Hamamura, N., Kataoka, T., Shiraishi, F., 2013. Arsenic attenuation in geothermal streamwater coupled with biogenic arsenic(III) oxidation. Appl. Geochem. 35, 154–160.
Moldovan, B.J., Jiang, D.T., Hendry, M.J., 2003. Mineralogical characterization of arsenic in uranium mine tailings precipitated from iron-rich hydrometallurgical solutions. Environ. Sci. Technol. 37, 873–879.
Morin, G., Calas, G., 2006. Arsenic in soils, mine tailings, and former industrial sites. Elements 2, 97–101.
Mukherjee, A., Sengupta, M.K., Hossain, M.A., Ahamed, S., Das, B., Nayak, B., Lodh, D., Rahman, M.M., Chakraborti, D., 2006. Arsenic contamination in groundwater: a global perspective with emphasis on the Asian scenario. J. Health Popul. Nutr. 24, 142–163.
Mulligan, C.N., Yong, R.N., 2004. Natural attenuation of contaminated soil. Environ. Int. 30, 587–601.
Nimick, D.A., Moore, J.N., Dalby, C.E., Savka, M.W., 1998. The fate of geothermal arsenic in the Madison and Missouri Rivers, Montana and Wyoming. Water Resour. Res. 34, 3051–3067.
Noh, H., Huh, Y., Qin, J., Ellis, A., 2009. Chemical weathering in the three rivers region of eastern Tibet. Geochim. Cosmochim. Acta 73, 1857–1877.
Nordstrom, D.K., 2002. Public health – worldwide occurrences of arsenic in ground water. Science 296, 2143–2145.
Nordstrom, D.K., 2012. Arsenic in the geophere meets the anthroposphere. Understanding the Geological and Medical Interface of Arsenic, pp. 15–19.
Nordstrom, D.K., Ball, J.W., McCleskey, R.B., 2005. Ground water to surface water: chemistry of thermal outflows in Yellowstone National Park. In: Geothermal Biology and Geochemistry in Yellowstone National Park, pp. 73–94.
O'Day, P.A., Vlassopoulos, D., Root, R., Rivera, N., 2004. The influence of sulfur and iron on dissolved arsenic concentrations in the shallow subsurface under changing redox conditions. In: Proceedings of the National Academy of Sciences of the United States of America, vol. 101, pp. 13703–13708.
Pan, J., 1999. Characteristics of sediment transportation in Jinsha river basin. J. Sediment Res. 46–49.
Parviainen, A., Lindsay, M.B.J., Perez-Lopez, R., Gibson, B.D., Ptacek, C.J., Blowes, D.W., Loukola-Ruskeeniemi, K., 2012. Arsenic attenuation in tailings at a former Cu-W-As mine, SW Finland. Appl. Geochem. 27, 2289–2299.
Planer-Friedrich, B., Fisher, J.C., Hollibaugh, J.T., Süß, E., Wallschläger, D., 2009. Oxidative transformation of trithioarsenate along alkaline geothermal drainages—abiotic versus microbially mediated processes. Geomicrobiol. J. 26, 339–350.
Planer-Friedrich, B., London, J., McCleskey, R.B., Nordstrom, D.K., Wallschläger, D., 2007. Thioarsenates in geothermal waters of Yellowstone National Park: determination, preservation, and geochemical importance. Environ. Sci. Technol. 41, 5245–5251.
Polizzotto, M.L., Kocar, B.D., Benner, S.G., Sampson, M., Fendorf, S., 2008. Near-surface wetland sediments as a source of arsenic release to ground water in Asia. Nature 454, 505–508.
Qin, H., Zhu, J., Li, S., Wang, M., 2010. Determination of total arsenic in environmental samples by hydride generation-atomic fluorescence spectrometry with PTFE Bomb. Acta Mineral. Sin. Chin. 30, 398–402.
Ravel, B., Newville, M., 2005. ATHENA, ARTEMIS, HEPHAESTUS: data analysis for X-ray absorption spectroscopy using IFEFFIT. J. Synchrotron Radiat. 12, 537–541.
Ravenscroft, P., Brammer, H., Richards, K., 2009. Arsenic Pollution: a Global Synthesis. John-Wiley & Sons, Oxford.
Rudnick, R.L., Gao, S., 2003. Composition of the continental crust. In: Rudnick, R.L., Holland, H.D., Turekian, K.K. (Eds.), The Crust. Elsevier-Pergamon, Oxford, pp. 1–64.
Saunders, J.A., Lee, M.K., Uddin, A., Mohammad, S., Wilkin, R.T., Fayek, M., Korte, N.E., 2005. Natural arsenic contamination of Holocene alluvial aquifers by linked tectonic, weathering, and microbial processes. Geochem. Geophys. Geosyst. 6.
Smedley, P.L., Kinniburgh, D.G., 2002. A review of the source, behaviour and distribution of arsenic in natural waters. Appl. Geochem. 17, 517–568.
Smith, A.H., Goycolea, M., Haque, R., Biggs, M.L., 1998. Marked increase in bladder and lung cancer mortality in a region of Northern Chile due to arsenic in drinking water. Am. J. Epidemiol. 147, 660–669.
Stanger, G., 2005. A palaeo-hydrogeological model for arsenic contamination in southern and south-east Asia. Environ. Geochem. Health 27, 359–367.
Strawn, D., Doner, H., Zavarin, M., McHugo, S., 2002. Microscale investigation into the geochemistry of arsenic, selenium, and iron in soil developed in pyritic shale materials. Geoderma 108, 237–257.
Ta, T.K.O., Nguyen, V.L., Tateishi, M., Kobayashi, I., Saito, Y., Nakamura, T., 2002a. Sediment facies and Late Holocene progradation of the Mekong River Delta in Bentre Province, southern Vietnam: an example of evolution from a tide-dominated to a tide-and wave-dominated delta. Sediment. Geol. 152, 313–325.
Ta, T.K.O., Nguyen, V.L., Tateishi, M., Kobayashi, I., Tanabe, S., Saito, Y., 2002b. Holocene delta evolution and sediment discharge of the Mekong River, southern Vietnam. Quat. Sci. Rev. 21, 1807–1819.
Tessier, A., Campbell, P.G.C., Bisson, M., 1979. Sequential extraction procedure for the speciation of particulate trace metals. Anal. Chem. 51, 844–850.
van Geen, A., Win, K.H., Zaw, T., Naing, W., Mey, J.L., Mailloux, B., 2014. Confirmation of elevated arsenic levels in groundwater of Myanmar. Sci. Total Environ. 478, 21–24.
Vodyanitskii, Y.N., 2006. Arsenic, lead, and zinc compounds in contaminated soils according to EXAFS spectroscopic data: a review. Eurasian Soil Sci. 39, 611–621.
Walker, S.R., Parsons, M.B., Jamieson, H.E., Lanzirotti, A., 2009. Arsenic mineralogy of near-surface tailings and soils: influences on arsenic mobility and bioaccessibility in the Nova Scotia gold mining districts. Can. Mineral. 47, 533–556.
Wang, E., Burchfiel, B.C., 2000. Late Cenozoic to Holocene deformation in

southwestern Sichuan and adjacent Yunnan, China, and its role in formation of the southeastern part of the Tibetan Plateau. Geol. Soc. Am. Bull. 112, 413–423.
Wang, J.-a., Xu, Q., Zhang, W.-r., 1990. Heat flow data and some geologic-geothermal problems in Yunnan Province. Seismol. Geol. Chin. 12, 367–377.
Waychunas, G.A., Rea, B.A., Fuller, C.C., Davis, J.A., 1993. Surface chemistry of ferrihydrite: Part 1. EXAFS studies of the geometry of coprecipitate and adsorbed arsenate. Geochim. Cosmochim. Acta 57, 2251–2269.
Webster-Brown, J.G., Lane, V., 2005. Modeling seasonal arsenic behavior in the Waikato River, New Zealand. In: Oday, P.A., Vlassopoulos, D., Meng, Z., Benning, L.G. (Eds.), Advances in Arsenic Research: Integration of Experimental and Observational Studies and Implications for Mitigation, pp. 253–266.
Webster, J.G., Nordstrom, D.K., 2003. Geothermal arsenic. In: Welch, A.H., Stollenwerk, K.G. (Eds.), Arsenic in Ground Water: Geochemistry and Occurrence. Kluwer Academic Publishers, Boston, pp. 101–126.
Wilkie, J.A., Hering, J.G., 1998. Rapid oxidation of geothermal arsenic(III) in streamwaters of the eastern Sierra Nevada. Environ. Sci. Technol. 32, 657–662.
Wilson, N., Webster-Brown, J., 2009. The fate of antimony in a major lowland river system, the Waikato River, New Zealand. Appl. Geochem. 24, 2283–2292.
Xu, Q., Li, C., Wang, J., Chen, M., 1997. Geothermal resources in Tengchong region, Yunnan province. Geol. Geochem. Chin. 77–84.
Zhang, G., Liu, C., Liu, H., Jin, Z., Han, G., Li, L., 2008. Geochemistry of the Rehai and Ruidian geothermal waters, Yunnan Province, China. Geothermics 37, 73–83.
Zhang, H., Selim, H.M., 2005. Kinetics of arsenate adsorption-desorption in soils. Environ. Sci. Technol. 39, 6101–6108.
Zhang, X., Deng, W., Yang, X., 2002. The background concentrations of 13 soil trace elements and their relationships to parent materials and vegetation in Xizang (Tibet), China. J. Asian Earth Sci. 21, 167–174.
Zhang, Z.-F., Zhu, M.-X., Liu, S.-B., Shao, H.-X., Chen, Y.T., 1982. Preliminary studies of hydrothermal geochemistry of Xizang (in Chinese with English abstract). Acta Sci. Nat. Univ. Pekin. 3, 88–96.
Zhao, P., Xie, E.J., Dor, J., Jin, J., Hu, X.C., Du, S.P., Yao, Z.H., 2002. Geochemical characteristics of geothermal gases and their geological implications in Tibet (in Chinese). Acta Petrol. Sin. 18, 539–550.
Zheng, Y., 2007. The heterogeneity of arsenic in the crust: a linkage to occurrence in groundwater. Quat. Sci. Chin. 27, 1–15.
Zheng, Y., Stute, M., van Geen, A., Gavrieli, I., Dhar, R., Simpson, H.J., Schlosser, P., Ahmed, K.M., 2004. Redox control of arsenic mobilization in Bangladesh groundwater. Appl. Geochem. 19, 201–214.
Zhou, Z.Y., Qin, C.L., 1991. Characteristic of hydrothermal activity and its relation with active structure in Tibet (in Chinese with English abstract). Xizang Geol. 1, 25–37.
Zhu, B., Zhu, L., Shi, C., Yu, H., Wang, G., 1989. Application of geochemical methods in the search for geothermal fields. J. Geochem. Explor. 33, 171–183.